Magnetic Sensor Design for Femtotesla Low-Frequency Signals

Sarah K. Harriman, *Student Member, IEEE*, Evans W. Paschal, and Umran S. Inan, *Fellow, IEEE*

***Abstract*—A system for detecting magnetic fields in the femtotesla range at low frequencies is developed, including the antenna, transformer, and amplifier. Each component is described with relevant tradeoffs which allow a large variety of receivers to be easily designed for any magnetic field sensing in the very low frequency range. A system using a 1-Ω–1-mH impedance antenna is developed further as an example that has been used extensively in measurements all over the world in the frequency range of 50 Hz–30 kHz. It has a gain of 0.58 V/nT and a sensitivity of below 1 fT/Hz$^{1/2}$ above 250 Hz.**

***Index Terms*—Amplifiers, loop antennas, magnetic field measurement, magnetometers.**

I. Introduction

MAGNETIC field receivers are used to sense low-frequency [(LF); < 30 kHz] electromagnetic waves because of their superior noise performance at low frequencies and their relative tolerance of nearby metallic structures compared to electric field sensors. Superconducting QUantum Interference Devices (SQUIDs) are commonly available amplifiers in this frequency range. These generally use a high-input impedance amplifier and then use feedback to reduce the input impedance as seen by the sensor ([1] and [2]). Although good noise performance is obtained, they must be operated below the critical temperature of the superconductors, near 0 K. In general, it is difficult to design a SQUID-based amplifier to have an input impedance as low as is required while remaining stable (see [3]).

In [4], a system designed for room temperature also uses a feedback topology; however, the noise performance suffers. Another system developed by Stuchly *et al.* [5] senses magnetic fields between 600 Hz and 210 MHz with a transformer between the sensor and the amplifier. However, they use not only a high-input impedance amplifier with feedback but also a shunt resistor to ground at the amplifier input. This shunt resistor increases the noise significantly and is used in applications where the noise is not a primary concern. In their case, noise measurements are not even reported.

In ground-based magnetospheric research, we are interested in receiving signals with large loop antennas from 300 Hz to 30 kHz. Natural signals in this frequency range include sferics and tweaks generated by lightning, whistlers created when sferics penetrate the ionosphere and travel along a magnetic field line to the other hemisphere, and chorus and hiss due to plasma instabilities in the magnetosphere. Man-made signals include those from the very LF (VLF) navigation and communications transmitters. Using these signals, we study the processes that occur during geomagnetic storms, aurorae, and what is now often called "space weather."

These signals have a more or less constant power spectral density from 300 Hz to 30 kHz; thus, we need the receiver to have a flat frequency response over this range rather than one, for example, proportional to frequency. If we use a receiver with a low input impedance, the increase in induced electromotive force in the antenna with frequency is counteracted by the increase in inductive reactance of the antenna, making the current into the receiver flat with frequency. The problem is to design a low-impedance amplifier with a good noise figure when connected to an inductive source. We have found that a common–base input stage gives good results, much better than, for example, terminating the loop with a resistor of the same impedance even if followed by an ideal noise-free amplifier.

In this paper, we describe a sensitive VLF receiver design method originally developed by E. Paschal. The various design equations and tradeoffs of the antenna, transformer, and low-noise amplifier are discussed. Section II begins by describing the design of the loop antenna. Next, we discuss the tradeoffs involved in the transformer design in Section III. Section IV follows, describing the amplifier design. In Section V, an example system using a 1-Ω–1-mH antenna design is presented, and the corresponding performance is shown in Section VI.

II. Antenna Design

Magnetic field antennas are large air-coil loops of wire with N_a turns and area A_a. Air loops are used instead of ferrite core loops for better linearity and reduced temperature dependence. When designing an air loop antenna, there are three parameters available: the area of the antenna, the diameter of the wire, and the number of turns. These parameters determine the antenna's wire resistance R_a and inductance L_a (see Fig. 1, left panel, for antenna impedance model), which, in turn, shape the system response and sensitivity. Winding capacitance and skin effect

Manuscript received January 14, 2008; revised November 14, 2008 and April 18, 2009. First published September 18, 2009; current version published December 23, 2009. This work was supported by the National Science Foundation's Office of Polar Programs under Grants 0840058, 0636927, and 0341165.

S. K. Harriman is with the Space, Telecommunications, and Radioscience Laboratory, Department of Electrical Engineering, Stanford University, Stanford, CA 94305-9505 USA (e-mail: harriman@stanford.edu).

E. W. Paschal is with Whistler Radio Services, Anderson Island, WA 98303 USA (e-mail: epaschal@att.net).

U. S. Inan is with the Space, Telecommunications, and Radioscience Laboratory, Department of Electrical Engineering, Stanford University, Stanford, CA 94305-9505 USA, and also with Koc University, Istanbul 34450, Turkey (e-mail: inan@nova.stanford.edu).

Color versions of one or more of the figures in this paper are available online at http://ieeexplore.ieee.org.

Digital Object Identifier 10.1109/TGRS.2009.2027694

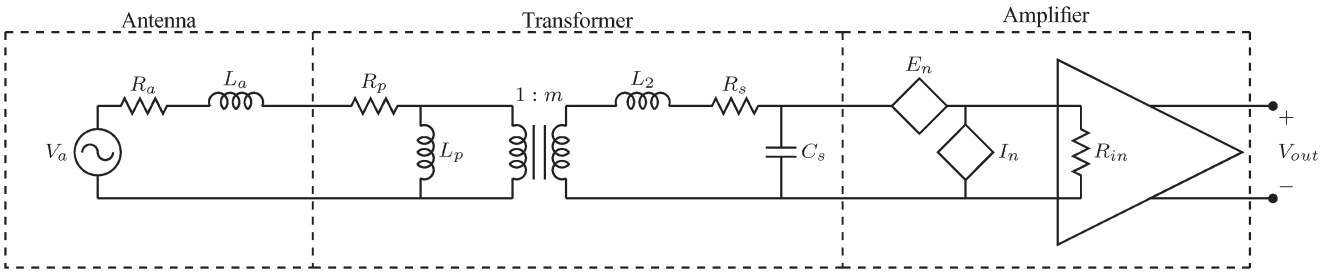

Fig. 1. System design of fully differential magnetic field receiver, including antenna model, transformer model, and noise model of amplifier.

TABLE I
CONSTANTS FOR VARIOUS MAGNETIC LOOP ANTENNA SHAPES

Shape of Loop	c_1	c_2
circular	3.545	0.815
regular octagon	3.641	0.925
regular hexagon	3.722	1.000
square	4.000	1.217
equilateral triangle	4.559	1.561
right isosceles triangle	4.828	1.696

are negligible at these frequencies. It is therefore important to derive the relationship among the three parameters and the resulting R_a, L_a, and sensitivity.

Loop shape is usually chosen based on its ease of construction given a desired area. A variety of common loop shapes available are listed in Table I. The constant c_1 is related to the geometry of the antenna and allows for a general expression of the length of each turn that is valid for any shape

$$Antenna\ Turn\ Length = c_1\sqrt{A_a}. \tag{1}$$

Using this expression, the antenna resistance for any shape is

$$R_a = \frac{4\rho N_a c_1\sqrt{A_a}}{\pi d^2} \tag{2}$$

where ρ is the resistivity of the wire (for copper, $\rho = 1.72 \times 10^{-8}$ Ωm), and d is the diameter of the wire. Adapting from [6, pp. 49–53], the inductance for any loop antenna is

$$L_a = 2.00 \times 10^{-7} N_a^2 c_1\sqrt{A_a}\left[\ln\frac{c_1\sqrt{A_a}}{\sqrt{N_a}d} - c_2\right] \tag{3}$$

where c_2 is also a geometry-related constant and can be found in Table I for a variety of loop shapes. The two variables R_a and L_a form the total impedance of the antenna (Z_a) that is the source impedance seen by the first stage of the receiver

$$Z_a = R_a + j\omega L_a. \tag{4}$$

When an incident electromagnetic wave passes through the antenna, the voltage induced across its terminals is given by Faraday's law

$$V_a = j2\pi f N_a A_a B\cos(\theta) \tag{5}$$

where f is the frequency, B is the magnetic flux density, and θ is the angle of the magnetic field from the axis of the loop. If the axis of the loop is horizontal, the response pattern of the antenna is a dipole in azimuth. In the following, we shall be concerned with the response of the loop to an appropriately oriented field and will omit the term $\cos(\theta)$.

Since a VLF receiving loop is very small compared to a wavelength ($\lambda = 1000$ km at 300 Hz and 10 km at 30 kHz), the radiation resistance of the loop is negligible compared to the wire resistance R_a. The minimum detectable signal is limited by the thermal noise of R_a. We define the sensitivity of the antenna S_a as the field equivalent of the noise density, i.e., the amplitude of an incident wave which would give an output voltage equal to the thermal noise of R_a in a 1-Hz bandwidth. Using (5), we can express the sensitivity (in units of T/Hz$^{1/2}$) as

$$S_a = \frac{\sqrt{4kTR_a}}{2\pi f N_a A_a}. \tag{6}$$

The antenna sensitivity S_a decreases with frequency (i.e., the antenna becomes more sensitive) at $1/f$. It is convenient to define a frequency-independent quantity for comparing the performances of different antennas. We define the normalized sensitivity as $\hat{S}_a = fS_a$. Using R_a in (2), we find an expression for the normalized sensitivity that depends only on the physical parameters of the antenna

$$\hat{S}_a = \frac{\sqrt{4kT\rho c_1}}{\pi^{3/2} d\sqrt{N_a}A_a^{3/4}}. \tag{7}$$

This expression for sensitivity can be used to find the number of turns, antenna area, and wire diameter required for a target sensitivity at a specific frequency. The effect of the resulting antenna resistance and impedance on the rest of the system is discussed in later sections.

Further insight can be gained by recalculating this sensitivity as a function of the mass of the antenna. The mass of the wire used in the antenna can be calculated as

$$M = \frac{1}{4}\pi\delta c_1 d^2\sqrt{N_a} \tag{8}$$

where δ is the density of the wire. Solving this for $d\sqrt{N_a}$ and substituting into (7) produce normalized sensitivity

$$\hat{S}_a = \frac{c_1\sqrt{4kT\rho\delta}}{2\pi\sqrt{MA_a}}. \tag{9}$$

This interesting result shows that the only way to improve sensitivity with a given antenna material is to increase the total mass or area of the antenna. These receivers are usually placed in remote areas to reduce interference from power lines (at 60 Hz and harmonics); thus, this fundamental tradeoff means that the sensitivity must be balanced against practical limitations regarding weight and size. The most severe limitations for

these receivers are units placed at the South Pole for research on the magnetosphere. Since the Earth's magnetic field lines that pass through these regions in the upper atmosphere cross the Earth's surface at the poles, it is the only place that a ground-based receiver can detect the LF signals that follow these field lines.

III. Transformer

The transformer electrically isolates the antenna from the rest of the receiver and steps up the impedance by a factor of the square of the turn ratio m^2 to improve the impedance match to the preamplifier. Moreover, the LF cutoff reduces the noise from the system at frequencies below those of interest. Fig. 1 shows the transformer model and the equivalent noise sources from the amplifier.

The combined transfer function of the antenna and transformer can be found with a standard circuit analysis

$$\frac{V_{\rm in}}{V_a} = \frac{jwmL_pR_{\rm in}}{k_1 * k_2 + k_3} \tag{10}$$

where

$$\begin{aligned} k_1 &= [R_a + R_p + jw(L_a + L_p)] \\ k_2 &= [(R_s + jwL_2)(1 + jwC_sR_{\rm in}) + R_{\rm in}] \\ k_3 &= jwL_pm^2(R_a + R_p + jwL_a)(1 + jwC_sR_{\rm in}). \end{aligned}$$

Using (5) and simplifying, the approximate equation shown as follows facilitates the understanding of how the transfer function is affected by both the design of the transformer and the input impedance of the amplifier:

$$V_{\rm in} \approx \frac{N_aA_aR_{\rm in}B}{m(L_a + pL_2/m^2)} \left[\frac{f}{f - jf_t}\right] \left[\frac{f}{f - jf_i}\right] \left[\frac{-jf_c}{f - jf_c}\right] \tag{11}$$

where

$$\begin{aligned} f_t &= \frac{(R_a + R_p) \| \left((R_s + R_{\rm in})p/m^2\right)}{2\pi(L_a + L_p)} \\ f_i &= \frac{R_a + R_p + (R_s + R_{\rm in})p/m^2}{2\pi\left(L_a + pL_2/m^2\right)} \\ f_c &= \frac{1}{2\pi C_sR_{\rm in}} \\ p &= 1 + L_a/L_p. \end{aligned}$$

The factor p is the ratio of the total inductance on the primary side (including the antenna and L_p) to the transformer primary inductance alone (L_p). For an ideal transformer, $L_p = \infty$, and $p = 1$. Below the frequency f_t, the shunting effect of L_p becomes important, and the gain drops rapidly. The receiver is not useful in this region, making f_t as the LF limit of the receiver response.

The input turnover frequency f_i is the frequency where the total resistance in the input circuit is equal to the inductive reactance. Note that f_i is much higher than f_t in a good design. Above f_i, the impedance of the input circuit is dominated by the antenna inductive reactance $2\pi fL_a$. Even though the induced voltage across the antenna terminals (5) is proportional to frequency, the current in the input circuit above f_i is limited by the antenna reactance, which also increases with frequency, giving a flat overall frequency response. This is desirable for most LF and VLF applications.

At the frequency f_c, the transformer secondary shunt capacitance C_s begins to short the input signal, and the gain drops. The interval of flat frequency response is thus from f_i to f_c. Note that the transformer leakage inductance L_2 does not significantly affect performance. That is because it appears in series with the much larger m^2L_a, as seen on the secondary side of the transformer.

The main sources of noise in the system are the thermal noise of the antenna (E_a), voltage noise of the amplifier (E_n), and the current noise of the amplifier (I_n). The noise sources from the amplifier E_n and I_n are assumed to be statistically uncorrelated. (This is usually true at audio frequencies; if they are correlated, the error is, at most, 30%.) The system sensitivity is directly affected by the transformer turn ratio and the ratio of current and voltage noise of the amplifier. For an ideal transformer

$$S_{\rm sys} = \frac{E_a^2 + E_n^2/m^2 + I_n^2m^2Z_a^2}{\omega N_aA_a}. \tag{12}$$

Since the effect of the amplifier noise voltage is reduced by the transformer turn ratio while that of the noise current is increased, the choice of turn ratio has a direct effect on the sensitivity. Typically, we choose m so that $R_a = R_{\rm in}/m^2$. That is, we choose the turn ratio so that the input impedance of the amplifier as seen at the transformer primary is about the same as the antenna resistance for a good balance between low- and high-frequency noise concerns. With a common–base input stage, this also gives $E_a^2 \approx E_n^2/m^2$, thus making the LF noise figure about 3 dB. With this choice, the sensitivity improves with higher frequency for a decade or two above f_i until the current noise I_n flowing through $m^2Z_a^2$ becomes important and the sensitivity levels off. Note that a common–base input stage of input resistance $R_{\rm in}$ gives much better noise performance than an actual resistor of size $R_{\rm in}$, even if followed by a noiseless amplifier. The reason is that the current noise of the common–base circuit is much lower than the Johnson thermal current noise of the real resistor.

However, a real transformer adds some noise and so changes the response. When the real transformer model is used, the total input-referred voltage noise is

$$\begin{aligned} E_{ni}^2 \approx{}& E_a^2 + E_p^2 + \frac{E_s^2}{m^2}p^2\left(1 + \frac{f_{tn}^2}{f^2}\right) \\ &+ \frac{E_n^2}{m^2}\left[\left(p - \frac{f^2}{f_{cn}^2}\right)^2 + p^2\frac{f_{tn}^2}{f^2}\right] \\ &+ I_n^2m^2R_a^2\left(1 + \frac{(2\pi fL_a)^2}{R_a^2}\right) \end{aligned} \tag{13}$$

where

$$\begin{aligned} f_{tn} &= \frac{R_a + R_p}{2\pi(L_a + L_p)} \\ f_{cn} &= \frac{1}{2\pi\sqrt{C_sm^2L_a}}. \end{aligned}$$

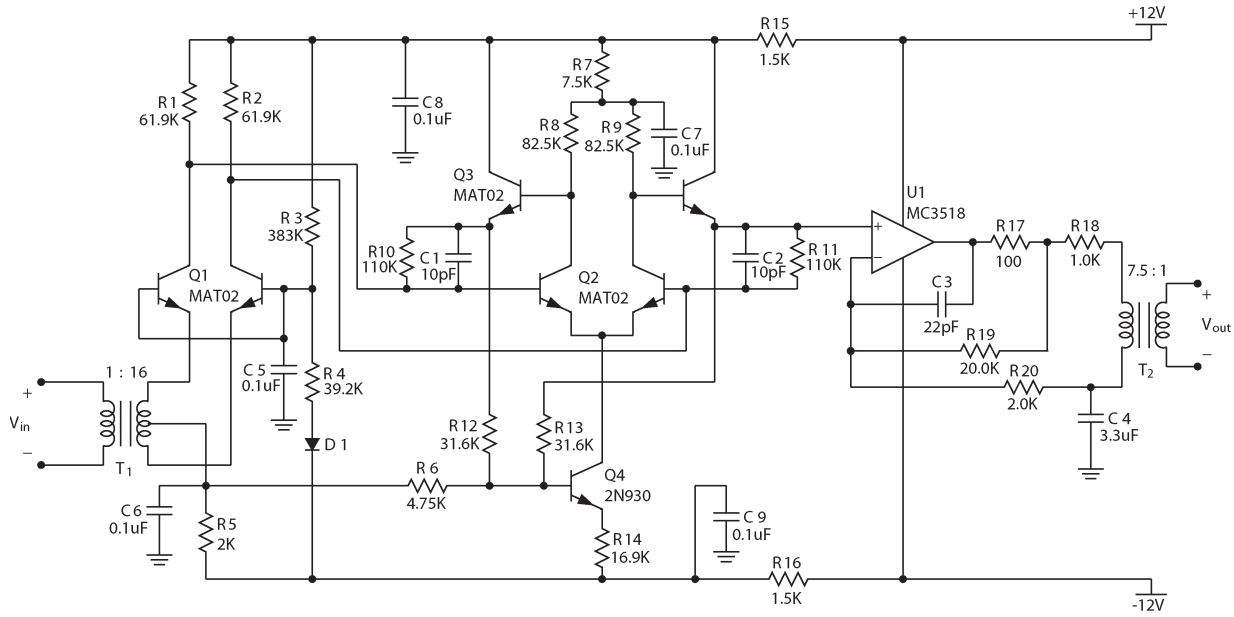

Fig. 2. Differential preamplifier circuit design showing input and output transformers, by D. Shafer and based on E. Paschal's original design. The common–base first stage provides a low-impedance input. The second stage provides gain, and the op-amp circuit drives a long cable (usually about 250 ft), allowing the digital electronics to be located far from the sensitive antenna.

To find the sensitivity, convert the input-referred noise to the equivalent field using the antenna parameters

$$S_{\rm sys} = \frac{E_{ni}}{\omega N_a A_a}. \tag{14}$$

Comparing this to (6), we see that the sensitivity of the system is similar in form to that of the antenna by itself. At a given frequency, the receiver approaches ideal performance as E_{ni} decreases toward E_a.

The transformer has several important effects on the overall noise. The most important effect is the series resistances in the transformer. The thermal noise of these resistances adds directly to the noise and so must be kept as small as possible. At low frequencies, $f^2/f_{cn}^2 \to 0$, and the voltage noise is multiplied by the factor p. Therefore, for good LF noise performance, p must be kept small (i.e., L_p made large). Moreover, at frequencies below f_{tn}, the noise performance deteriorates rapidly; thus, f_{tn} must be kept small. At high frequencies, more of the amplifier voltage noise appears across the transformer capacitance C_s and increases the noise. Therefore, for good high-frequency noise performance, f_{cn} should be kept large.

It is important to note that the transformer design depends on the impedances and noise characteristics of both the antenna and amplifier. This requires that the system be designed as a unit (antenna, transformer, and amplifier) to produce the desired frequency response and sensitivity.

IV. Amplifier

The amplifier has many unique requirements that require a custom design. The first requirement comes from the definition of f_i from (11). Assuming an ideal transformer for simplicity (resistances $\to 0$, $L_p \to \infty$, and $L_2 \to 0$), f_i becomes

$$f_i = \frac{R_a + R_{\rm in}/m^2}{2\pi L_a} \tag{15}$$

which shows that, as $R_{\rm in}$ is reduced, the useful bandwidth of the receiver increases. The other main requirement of this receiver involves the noise. Not only do the noise components need to be as small as possible but also the ratio of the voltage noise and current noise is important [see (12)]. In addition, because of the very low frequencies, dc feedback loops are used to maintain the needed voltage levels instead of decoupling capacitors.

Many previous circuit solutions for matching to a low-impedance sensor involve using a high-impedance amplifier with negative feedback. However, in this case, the sensor impedance is so low (256 Ω at low frequencies, as seen from the secondary of the transformer) that this option is not feasible. The feedback resistance would create its own current noise that adds to the input. As this resistance is increased to reduce the noise, the gain of the amplifier must be increased to keep the input impedance the same. This creates an amplifier of such high gain that stability becomes a serious concern.

A simpler solution is to use a common–base or common–gate input stage because of their low input impedances, as shown with device Q1 in Fig. 2. Bipolar junction transistors (BJTs) were chosen because their input impedance is more consistent than that of MOSFETs in which the common-gate impedance $1/g_m$ can have a large spread between individual discrete devices. It is also important that the specific transistor parts chosen have very low noise. In addition, the input stages remain differential to reduce the second harmonic distortion. The input impedance of the differential first stage is twice the input impedance of a common–base BJT

$$R_{\rm in} = 2r_e = 2\frac{kT}{qI_E}. \tag{16}$$

Therefore, the collector current of the input stage BJTs can be used to adjust $R_{\rm in}$ as desired.

The dc current also directly affects the voltage and current noise of the transistors. From [7, p. 116], the voltage noise of a

BJT is

$$E_n^2 = 4kTr_b + \frac{2(kT)^2}{qI_C} \tag{17}$$

where r_b is the base resistance. The current noise includes both shot noise and $1/f$ noise

$$I_n^2 = 2qI_B + \frac{2qI_C}{\beta^2} + \frac{KI_B^\gamma}{f^\alpha}. \tag{18}$$

However, the chosen input transistor part should have low enough $1/f$ noise that shot noise dominates. Both the current and voltage noise depend on the collector current; thus, there is a tradeoff between the desired input impedance $R_{\rm in}$ and the noise performance.

The current noise for the second-stage BJTs (Q2) is also given by (18). Because the current gain of the first stage is one, second-stage current noise is important and appears as if it was in parallel with the first-stage current noise at the amplifier input. To minimize this additional noise, the second stage is operated at a lower collector current, roughly one-third of the current of the first stage.

The second-stage Q2 is a standard differential pair. The voltage–follower pair Q3 prevents the loading of the high-impedance outputs at the collectors of Q2. The tail current for Q2 is controlled by Q4. Resistors R10 and R11 give negative feedback around the second stage. The voltage gain from the transformer secondary to the input of the operational amplifier (op-amp) is $\mathrm{R10}/r_e$, where r_e is the input impedance of the common–base transistors Q1. Capacitors C1 and C2 provide compensation to ensure stability and limit the bandwidth to 150 kHz.

Proximity to power lines and digital equipment can couple noise into the antenna and prohibit sensitive measurements. In our experience, even the ticking of digital watches can be clearly seen in the recorded data. For this reason, the analog-to-digital converter, storage, and power supplies are located $\sim$200 ft from the antenna and preamplifier with a 78-Ω cable connection. The op-amp (U1) drives this line with the help of the step-down transformer (T2). These combine to produce a 1-V maximum signal that can travel to the system recorder. The transformer also provides dc isolation and a differential signal to preserve signal integrity along the long cable.

V. Example Design

The antenna design must balance the desired sensitivity with the practicality of construction. The resistance and inductance of the antenna from (2) and (3) affect the frequency response and sensitivity (11) and (13). For this design, we have chosen a 1-Ω–1-mH antenna impedance. The ratio gives f_i about 300 Hz, as desired [see (15)], and the impedance level lends itself to simple loop construction. In fact, using (3) and (6), we find that there is a family of copper-wire loops of various sizes and sensitivities, all with the same impedance. These antennas, listed in Table II, can be interchanged and used with the same receiver, depending on the sensitivity required. Similar tables can be constructed for other impedances.

TABLE II
Magnetic Field Antenna Designs With 1-Ω–1-mH Impedance

Base (m)	Wire AWG	N_a	R_a (Ω)	L_a (mH)	A_a (m^2)	$\hat{S_a}$ ($V\sqrt{Hz}/m$)
Square Antenna						
0.0160	20	47	1.002	0.998	.02563	5.03×10^{-3}
0.0567	18	21	1.006	0.994	.3219	8.96×10^{-4}
1.70	16	11	0.987	1.013	2.892	1.89×10^{-4}
4.90	14	6	0.972	1.029	24.05	4.13×10^{-5}
Right Isosceles Triangle						
2.60	16	12	0.994	1.005	1.695	2.97×10^{-4}
8.39	14	6	1.004	0.996	17.59	5.74×10^{-5}
27.3	12	3	1.035	0.967	187.0	1.10×10^{-5}
60.7	10	2	0.959	1.043	920.9	3.22×10^{-6}
202	8	1	1.005	0.995	10164	5.97×10^{-7}

The smaller antennas are more portable, while the large antennas are more sensitive; thus, the antenna choice is dependent upon the needed sensitivity and available physical space. For example, a small antenna can be used with a receiver system to determine the best low-noise site to construct a permanent large antenna. However, not only are large antennas heavy and difficult to construct in remote areas but wind can also cause vibrations that can be mistaken for data. Large antennas should use a stiff frame to keep wind vibrations small. For large open triangular antennas supported by a central tower, the antenna wire should be kept slack so that wind vibrations are below the frequencies of interest.

The transformer for this antenna has a turn ratio (m) of 16 and a primary inductance (L_p) of 10 mH. The high-frequency response is dominated by a winding capacitance C_s of 950 pF. This capacitance is high because bifilar winding is used in both the transformer primary and secondary windings to assure balanced coupling. Using single-strand winding, C_s can be much smaller. The following parameters' values were calculated as described in Section III:

$$\begin{aligned} p &= 1.10 & f_t &= 7.62 \text{ Hz} \\ f_i &= 320 \text{ Hz} & f_c &= 647 \text{ kHz}. \end{aligned} \tag{19}$$

Moreover, for the noise performance of the transformer, the LF noise corner f_{tn} is 14.5 Hz, and the high-frequency corner f_{cn} is 10.2 kHz.

The preamplifier circuit design shown in Fig. 2 also includes the component values and part numbers used in the example design. The first stage uses 200 μA for an $R_{\rm in}$ value of 259 Ω. The MAT02 transistors are used for their low $1/f$ noise, so that only shot and thermal noises dominate the receiver noise. The corresponding measurements for this example design are in the next section.

VI. Receiver Measurements

When taking measurements of these receivers in the lab, it is impractical to connect an antenna to the transformer and produce a known field that is constant across the span of the antenna. In addition, the very sensitive antennas will pick up so much environmental noise (particularly from power lines) that the amplifier will be constantly saturated. A better approach is to use a dummy antenna which has the same impedance as the antenna but no collecting area. In Fig. 3, we show the dummy

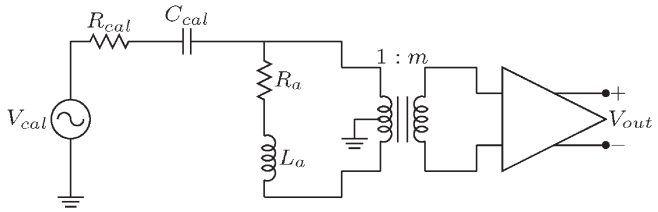

Fig. 3. Test setup using a dummy loop instead of antenna. This method allows for accurate lab testing and calibration.

antenna design used for testing. The antenna impedance is provided by R_a and L_a, while $R_{\rm cal}$ and $C_{\rm cal}$ are chosen by the following derivation.

The current flowing in the amplifier (secondary of transformer) from the source $V_{\rm cal}$ is

$$I_{\rm in} = \frac{V_{\rm cal}}{2R_{\rm cal}\left(1 + f_{\rm cal}/(jf)\right)} * \frac{j2\pi f L_a(1 + R_{\rm in}/j2\pi f L_a)}{R_a + j2\pi f L_a + Z_p}$$

where

$$f_{\rm cal} = \frac{1}{2\pi R_{\rm cal} C_{\rm cal}}$$

and Z_p is the impedance on the primary side of the transformer looking into the amplifier. The current produced by the antenna voltage V_a is

$$I_{\rm in} = \frac{V_a}{R_a + j2\pi f L_a + Z_p} = \frac{j2\pi f N_a A_a B}{R_a + j2\pi f L_a + Z_p}. \tag{20}$$

If these two input currents are equated, the relation between $V_{\rm cal}$ and V_a is found

$$V_{\rm cal} = \frac{2N_a A_a R_{\rm cal} B}{L_a} * \frac{1 + f_{\rm cal}/(jf)}{1 + (2\pi L_a)/(jfR_a)}. \tag{21}$$

If $C_{\rm cal}$ is chosen as follows:

$$C_{\rm cal} = \frac{L_a}{R_a * R_{\rm cal}} \tag{22}$$

and (5) is used to replace V_a, the relationship between $V_{\rm cal}$ and an equivalent magnetic field can be found

$$V_{\rm cal} = \frac{2N_a A_a R_{\rm cal} B}{L_a}. \tag{23}$$

Note that all of the terms with Z_p have dropped out, leaving a simple calibration method that does not require any knowledge of the impedance of the transformer and amplifier. Only the impedance and area of the antenna are relevant.

The measurements shown in this section were done using a dummy loop, as described earlier, and assuming an example square 1-Ω–1-mH antenna that is 4.9 m long with six turns (see Table II). The gain measurements in Fig. 4 are displayed as output voltage versus input magnetic field. The system has a flatband between 1 and 30 kHz, but has been routinely used for signals down to 100 Hz for geophysics research.

The sensitivity, as shown in Fig. 5, is below 1 fT/Hz$^{1/2}$ over most of the usable frequency range. Also plotted is the sensitivity obtained when the input is terminated with a 259-Ω resistor

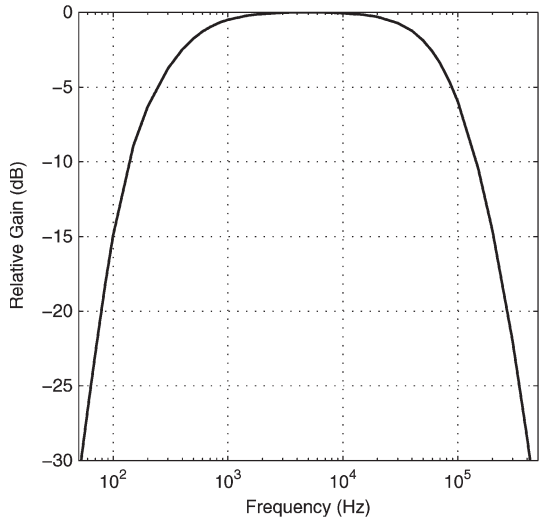

Fig. 4. System gain for an example design using a six-turn 4.9-m square loop antenna. Maximum gain is 0.58 V/nT.

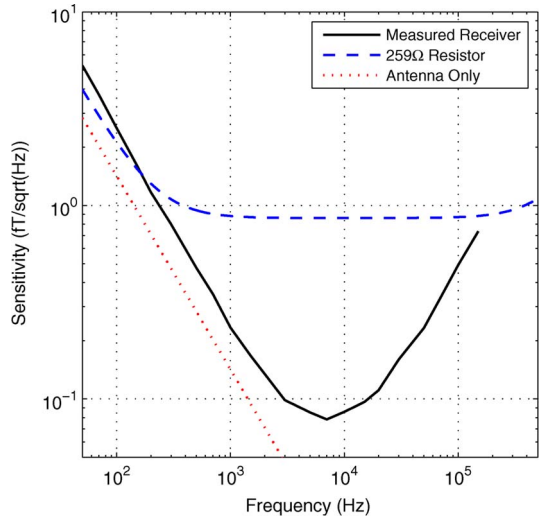

Fig. 5. System sensitivity for an example design using a six-turn 4.9-m square loop antenna comparing the measured receiver noise, the 1-Ω–1-mH antenna only, and a resistor with noiseless amplifier model. The resistor has much worse performance for the same input impedance than the common–base transistor input stage does.

(the input impedance of the amplifier circuit), followed by an ideal noiseless amplifier. The advantage of the common–base stage is clear. The noise of the system is dominated by the shot noise in the amplifier, but the shape of the sensitivity curve is determined by the frequency response of the antenna and transformer.

VII. Conclusion

A method of designing an LF receiver has been shown, including the antenna, transformer, and circuit design. The concepts described can be used to design and build a variety of antenna shapes, sizes, and impedances as desired. The transformer and amplifier input impedances can then be optimized for gain and noise. An example using a square 1-Ω–1-mH antenna has also been developed. Any shape and size of antenna that has this impedance can be used with the same transformer

and amplifier, allowing for a variety of sensitivity and convenience options without having to make any design changes. With this system, we have been able to detect signals in the femtotesla range at quiet sites from remote tropical islands to the South Pole.

REFERENCES

[1] T. Eriksson, "A SQUID picovoltmeter working at 77 K," *IEEE Trans. Appl. Supercond.*, vol. 9, no. 2, pp. 3495–3498, Jun. 1999.

[2] J. Lepaisant, M. L. C. Sing, and D. Bloyet, "Low-noise preamplifier with input feedback transformers for low source resistance sensors," *Rev. Sci. Instrum.*, vol. 63, no. 3, pp. 2089–2094, Mar. 1992.

[3] R. Sklyar, "Induction magnetic field transducers stability limits," *IEEE Sensors J.*, vol. 5, no. 5, pp. 924–928, Oct. 2005.

[4] J. Wikswo, P. Samson, and R. Giffard, "A low-noise low input impedance amplifier for magnetic measurements of nerve action currents," *IEEE Trans. Biomed. Eng.*, vol. BME-30, no. 4, pp. 215–221, Apr. 1983.

[5] M. Stuchly, H. LePoncher, D. T. Gibbons, and A. Thansandote, "Active magnetic field sensor for measurements of transients," *IEEE Trans. Electromagn. Compat.*, vol. 33, no. 4, pp. 275–280, Nov. 1991.

[6] F. Terman, *Radio Engineers' Handbook*. New York: McGraw-Hill, 1943.

[7] C. D. Motchenbacher and J. A. Connelly, *Low-Noise Electronic System Design*. Hoboken, NJ: Wiley, 1993.

Sarah K. Harriman (S'98) received the B.S. degree in electrical engineering from North Carolina State University, Raleigh, in 2000 and the M.S. degree from Stanford University, Stanford, CA, in 2003, where she is currently working toward the Ph.D. degree in electrical engineering in the Space, Telecommunications and Radioscience Laboratory, Department of Electrical Engineering.

Her research activity includes analog amplifier design for low-frequency applications. These amplifiers must use minimal power, be physically small, and tolerate extreme temperatures.

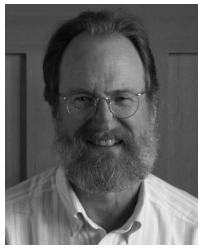

Evans W. Paschal received the B.A. degree in physics from Reed College, Portland, OR, in 1968 and the M.S. and Ph.D. degrees in electrical engineering from Stanford University, Stanford, CA, in 1969 and 1988, respectively, the latter for the study of phase characteristics of magnetospheric whistler-mode signals from the very low frequency (VLF) transmitter at Siple Station, Antarctica.

He was a Research Associate with the VLF Group, STARLab, Stanford University, from 1976 to 1986. In 1992, he started Whistler Radio Services, which is a consulting business on Anderson Island, WA. He has 40 years of experience in the design and operation of instruments for magnetospheric research. He has developed novel broadband extremely low frequency and VLF radio receivers and computerized recording and signal analysis equipment. He has made numerous trips to field stations in Antarctica and elsewhere in support of this research.

Dr. Paschal is a member of the American Geophysical Union, Sigma Xi, and the American Association for the Advancement of Science.

Umran S. Inan (S'76–M'77–SM'99–F'06) was born on December 28, 1950 in Turkey. He received the B.S. and M.S. degrees in electrical engineering from the Middle East Technical University, Ankara, Turkey, in 1972 and 1973, respectively, and the Ph.D. degree in electrical engineering from Stanford University, Stanford, CA, in 1977.

He is currently a Professor of electrical engineering with the Department of Electrical Engineering, Stanford University, where he serves as the Director of the Space, Telecommunications, and Radioscience Laboratory. He actively conducts research in electromagnetic waves in plasmas, lightning discharges, ionospheric physics, and very low frequency remote sensing. He has served as the Principal Ph.D. Dissertation Advisor for 28 students.

Dr. Inan is a member of Tau Beta Pi, Sigma Xi, and the Electromagnetics Academy. He is a Fellow of the American Geophysical Union. He is the recipient of the 2007 Stanford University Allan V. Cox Medal for Faculty Excellence in Fostering Undergraduate Research and in 1998 the Stanford University Tau Beta Pi Award for Excellence in Undergraduate Teaching. He has served as the Chair of the United States National Committee of the International Union of Radio Science (URSI) and the International Chair of Commission H (Waves in Plasmas) of URSI.